Diverse Human V_H antibody fragments with bio-therapeutic properties from the Crescendo Mouse

Yumin Teng, Joyce L. Young, Bryan Edwards, Philip Hayes, Lorraine Thompson, Colette Johnston, Carolyn Edwards, Yun Sanders, Michele Writer, Debora Pinto, Yanjing Zhang, Mila Roode, Peter Chovanec, Louise Matheson, Anne E Corcoran, Almudena Fernandez, Lluis Montoliu, Beatrice Rossi, Valentina Tosato, Kresimir Gjuracic, Dmitri Nikitin, Carlo Bruschi, Brian McGuinness, Thomas Sandal, Mike Romanos

PII: S1871-6784(19)30320-6

DOI: https://doi.org/10.1016/j.nbt.2019.10.003

Reference: NBT 1209

To appear in: *New BIOTECHNOLOGY*

Received Date: 25 June 2019

Revised Date: 4 September 2019

Accepted Date: 4 October 2019

Please cite this article as: Teng Y, Young JL, Edwards B, Hayes P, Thompson L, Johnston C, Edwards C, Sanders Y, Writer M, Pinto D, Zhang Y, Roode M, Chovanec P, Matheson L, Corcoran AE, Fernandez A, Montoliu L, Rossi B, Tosato V, Gjuracic K, Nikitin D, Bruschi C, McGuinness B, Sandal T, Romanos M, Diverse Human V_H antibody fragments with bio-therapeutic properties from the Crescendo Mouse, *New BIOTECHNOLOGY* (2019), doi: https://doi.org/10.1016/j.nbt.2019.10.003

Diverse Human V_H antibody fragments with bio-therapeutic properties from the Crescendo Mouse

Yumin Teng[a,§,*], Joyce L. Young[a,§,1], Bryan Edwards[a,§,2], Philip Hayes[a], Lorraine Thompson[a], Colette Johnston[a], Carolyn Edwards[a], Yun Sanders[a,3], Michele Writer[a,4], Debora Pinto[a,5], Yanjing Zhang[a,6], Mila Roode[a,7], Peter Chovanec[b], Louise Matheson[b], Anne E Corcoran[b], Almudena Fernandez[c], Lluis Montoliu[c], Beatrice Rossi[d], Valentina Tosato[d], Kresimir Gjuracic[d,8], Dmitri Nikitin[d], Carlo Bruschi[d], Brian McGuinness[a], Thomas Sandal[a,9] and Mike Romanos[a,10].

[a]Crescendo Biologics Ltd, Babraham Research Campus, Cambridge, CB22 3AT, UK

[b]Babraham Institute, Babraham Research Campus, Cambridge CB22 3AT, UK

[c]Centro Nacional de Biotecnologia (CNB-CSIC) & CIBER de Enfermedades Raras (CIBERER-ISCIII), Darwin 3, 28049 Madrid, Spain

[d]International Centre for Genetic Engineering and Biotechnology, Yeast Molecular Genetics Laboratory, Padriciano 99, 34149 Trieste, Italy

*Corresponding author

[1] Present address: Abcam PLC, Discovery Drive, Cambridge Biomedical Campus, Cambridge, CB2 0AX, UK.

[2] Present address: Antikor Ltd, Stevenage Bioscience Catalyst, Gunnels Wood Road, Stevenage, Herts SG1 2FX, UK.

[3] Present address: RxBiologics Ltd, Babraham Research Campus, Cambridge, CB22 3AT, UK.

[4] Present address: Avacta Life Sciences Ltd, Unit B, 1 Lion Works, Station Road, Whittlesford, Cambridge, CB22 4WL, UK.

[5] Present address: FairJourney Biologics, Rua do Campo Alegre 823 4150-180 Porto Portugal.

[6] Present address: bioMérieux Shanghai Co Limited, 4633 Pusan Road, Kangqiao Industrial Park, Pudong, 201315, Shanghai, China.

[7] Present address: Royal Liverpool University Hospital, Prescott Street, Liverpool L7 8XP, UK

[8] Present address: Gnosis by Lesaffre, Via Lavoratori Autobianchi 1, 20832 Desio, Italy

[9] Present address: AGC Biologics, Vandtaarnsvej 83B, DK-2860 Soeborg, Copenhagen, Denmark

[10] Present address: Microbiotica Limited, Biodata Innovation Centre, Wellcome Genome Campus, Cambridge CB10 1DR, UK.

[§] Joint first authors - these authors contributed equally to this paper

Graphical abstract

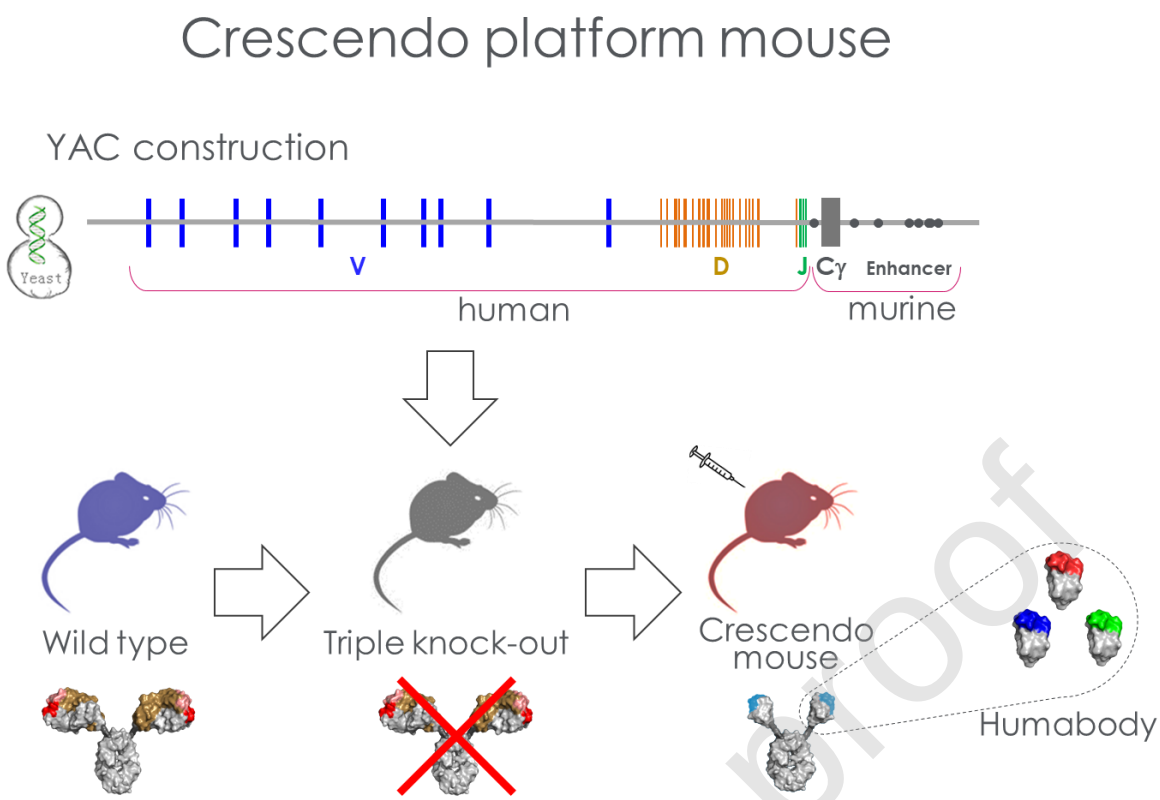

Highlights

- Crescendo Mouse produces heavy chain only antibodies with fully human variable domains.
- Triple knock out background is essential for *in vivo* maturation of HC-only antibody.
- Crescendo Mouse shows robust responses to immunisation generating high affinity Humabody® V_H against therapeutically relevant targets.
- Humabody® V_H fragments possess desirable biophysical properties for therapeutic development.

ABSTRACT

We describe the 'Crescendo Mouse', a human V_H transgenic platform combining an engineered heavy chain locus with diverse human heavy chain V, D and J genes, a modified

mouse Cγ1 gene and complete 3' regulatory region, in a triple knock-out (TKO) mouse background devoid of endogenous immunoglobulin expression. The addition of the engineered heavy chain locus to the TKO mouse restored B cell development, giving rise to functional B cells that responded to immunization with a diverse response that comprised entirely 'heavy chain only' antibodies. Heavy chain variable (V_H) domain libraries were rapidly mined using phage display technology, yielding diverse high-affinity human V_H that had undergone somatic hypermutation, lacked aggregation and showed enhanced expression in *E. coli*. The Crescendo Mouse produces human V_H fragments, or Humabody® V_H, with excellent bio-therapeutic potential, as exemplified here by the generation of antagonistic Humabody® V_H specific for human IL17A and IL17RA.

List of abbreviations:

BAC: Bacterial artificial chromosome

BIT: Bridge-induced translocation

CDR: Complementarity determining region

enh: Enhancer

HC: Heavy chain

IMAC: Immobilized metal affinity chromatography

IMGT: The international ImMunoGeneTics information system

IVF: *in vitro* fertilization

LC: Light chain

PBS: Phosphate buffered saline

SHM: Somatic hypermutation

Tg: Transgenic

TKO: Triple knock-out

V_H: Heavy chain variable domain

YAC: Yeast artificial chromosome

Keywords: heavy chain antibody; variable domain; V_H domain; Crescendo Mouse; Humabody® V_H.

Introduction

The market for monoclonal antibody (mAb) therapeutics has grown significantly since the approval of the first mAb therapeutic in 1986. It exceeded US$98 billion in sales amongst 22 active companies in 2017 with a future valuation of US$137-200 billion by 2022 0. Within this growth area, a major contribution has been made by the development of transgenic (Tg) mice in which human immunoglobulin (Ig) genes have been introduced to create a B cell repertoire that can be mined for therapeutics following immunisation with target antigens [2,3]. More recently, improvements to these Tg platforms have been leveraged by combining the entire human V region with murine constant region genes, thereby creating chimeric Ig molecules and restoring proper interactions with the murine B cell signalling capabilities through optimal engagement of the necessary Ig constant (C) region co-receptors [4-9]. These platforms combine the use of human genes with the power of *in vivo* affinity maturation to deliver chimeric mAbs that may be re-engineered with a human C-region to provide potent candidate human mAb therapeutics.

In addition to conventional Ig molecules, smaller formats are also being developed, such as antigen binding fragments (Fabs) and single chain variable fragments (scFv) [10,11]. The engineering of smaller antibody fragments has shown an improved rate of tumour uptake and intratumoral distribution [reviewed in 12,13]. The smallest functional antibody fragments, single variable domains, have recently attracted increasing attention for their therapeutic potential. Evidence that they can function as candidate therapeutics has come from both an *in vitro* phage display platform using a single human V_H scaffold such as V_H3-23 0 and from camelids where, using a limited set of distinct camelid genes, naturally occurring heavy-

chain (HC) only antibodies are made *in vivo* alongside conventional H_2L_2 antibodies with paired heavy and light chains 0. The camelid HC variable domains, termed V_{HH}, can be cloned from immunised llamas or camels and re-engineered to partially humanise them and create therapeutic products, termed Nanobodies® 0. Recently a Tg rat platform, 'UniRat', has been reported for development of human HC or single domain antibodies 0. Single domain fragments are expected to outperform mAbs for certain applications due to their small size resulting in better tissue and tumour penetration, rapid configuration for multi-specificity or multivalency and alternative routes of administration [18,19].

Here, the development is reported of a Tg mouse, termed 'Crescendo Mouse', that harnesses the power of an *in vivo* platform together with diverse human V_H gene usage, representing every major family framework, from which human V_H candidate therapeutics, termed Humabody® V_H, can be directly mined. Humabody® V_H molecules are human, lack synthetic mutations and, because they develop *in vivo* without a light chain (LC), possess exceptional biophysical characteristics (including but not limited to solubility and stability). The platform has generated hundreds of lead Humabody® V_H for multiple therapeutic targets. The potential of the Crescendo Mouse to deliver candidates for natural next-generation therapeutics is exemplified here by the generation of high potency, antagonistic Humabody® V_H to human Interleukin (IL)17A and its receptor IL17RA.

Materials and methods

Generation of yeast artificial chromosome (YAC) construct for transgenesis

The starting materials for transgene construction were a starter YAC (sYAC) kindly provided by Dr Marianne Brüggemann (Babraham Institute, Cambridge UK) comprising the first functional 5 human V_H genes and downstream D and J genes, combined with a human µ enhancer (Eµ), human µ switch (Sµ), and a human constant γ4 gene lacking the CH1 exon, and 3 bacterial artificial chromosomes (BACs): RP11-659B19; RP23-354L16 and RP24-72M1 (Supplementary Materials and Methods). Circular BAC RP11-659B19 was converted

into a linear YACa by Transformation-Associated Recombination (TAR) cloning 0 containing V3-7, V1-8, V3-9, V3-11 and V3-13 (**Figure 1**a). The V genes encoded by YACa and sYAC were combined using the bridge-induced chromosome translocation (BIT) technique 0 generating a new YAC encoding 10 human V_H genes (YACb, Figure 1b). The conversion of BAC to YAC and joining two YACs are detailed in Supplemental Materials and Methods. Four overlapping fragments were designed to replace the human Eμ-Cγ4 gene in YACb with a mouse Eμ-Cγ1 gene with deleted CH1 domain, using the yeast ability to recombine multiple DNA fragments with homologous sequences at the ends 0 (Supplementary Materials and Methods). A 4Kb YAC arm with the *LEU2* gene marker was generated by digestion of pYNOT (pYAC3 derivative replacing *URA3* with *LEU2*) with PshAI and BamHI restriction enzymes. These 5 overlapping fragments were introduced into the yeast *(Saccharomyces cerevisiae*) YLBW1 strain containing YACb by yeast spheroplast transformation 0 and cultured with selectable tryptophan and leucine drop-out medium. Successful homologous recombination between the overlapping fragments resulted in YACc with the replacement of human Eμ and Cγ4 with mouse Eμ and Cγ1 (Figure 1c). Finally, the murine 3' enhancer (3' enh) in BAC RP24-72M1 was cloned into a plasmid and joined to the end of murine Cγ1 of YACc by yeast recombination resulting in the addition of the murine 3' enh region and the Hyg-*HIS3*-telomere arm to generate the final 10V YAC construct (Figure 1d). The constructions are described in detail in Supplementary Materials and Methods, and primers used are listed in Supplementary Tables 1 and 2.

Generation of transgenic Crescendo Mouse with triple knock-out background

The 10V YAC was introduced into freshly fertilised oocytes of wild type (wt) B6B2F2 mice by pronuclear micro-injection (YAC DNA concentration: 1 ng/μl) and transferred into pseudo-pregnant females as described 0 to produce Tg founders with the intact YAC construct randomly integrated (Figure 1e). PCR analysis was performed to confirm presence of the transgene and onward germline transmission with primers listed in Supplementary Table 3. Mice silenced for endogenous heavy or light chain expression [25-27] were backcrossed to

generate triple knock-out (TKO) mice, confirmed by DNA genotyping (data not shown). The founder Tg mice were back-crossed in a two-stage breeding scheme with the TKO animals to create the Crescendo Mouse. Briefly, a Tg/wt mouse was cross-bred with TKO mates and sperm was collected from a male offspring with a quadruple heterozygous genotype ($Tg^{+/-}$ $HC^{+/-}\kappa^{+/-}\lambda^{+/-}$) and used to fertilise more than 1000 oocytes derived from superovulated TKO females ($Tg^{-/-}HC^{-/-}\kappa^{-/-}\lambda^{-/-}$). These were transferred freshly to pseudo-pregnant recipients or transferred after cryopreservation. From 65 recipients, a total of 405 pups were born and 22 of these were found to be $Tg^{+/-}$/TKO, consistent with the Mendelian inheritance pattern for four independently segregating loci.

Flow Cytometry

Single cell suspensions were prepared from bone marrow and spleen and following blocking with Fc fragments (012-0103; Rockland, Limerick, PA, USA), stained in FACS buffer (PBS/1%BSA/0.01%NaN_3) with antibodies to surface marker or isotype controls. Details of the antibodies used are provided in Supplementary Table 4. Following staining, cells were fixed with 3.7% formaldehyde solution and analysed by flow cytometry (BD LSRFortessa, BD, NJ, USA).

Deep sequencing analysis of Crescendo Mouse V_H repertoires

Deep sequencing of the naïve (non-immunised) Crescendo Mouse repertoire was performed by VDJ-seq methodology 0 and by GENEWIZ (NJ, USA). Plasmid DNA was purified from a phagemid library (constructed from spleen and lymph node samples, see below) and sequenced in two directions using Illumina Miseq 2x300bp chemistry and primers specific for the phagemid vector backbone. Raw sequencing data was subjected to data filtering and quality control and paired reads assembled into single fragments based on overlapping bases. The assembled sequences were analysed by CLC Main Workbench software (Qiagen, CA, USA) to determine CDR3 length, frequency and amino acid residue composition.

Immunisation of the Crescendo Mouse

Crescendo Mice, aged 8-12 weeks, were immunised with recombinant human IL17A (Peprotech, AF200-17), recombinant human IL17RA-Fc (R&D systems, 177-IR-100), Keyhole Limpet Haemocyanin (KLH, Calbiochem, 374811) or Ovalbumin (OVA, Sigma-Aldrich, A5503). Each mouse received a total of 10µg of recombinant protein, emulsified in Complete Freund's Adjuvant and delivered subcutaneously, followed by boosts at various intervals up to 49 days following the initial priming. Each boost was typically 1–10µg of recombinant protein, emulsified in Incomplete Freund's Adjuvant, administered subcutaneously, with a final dose of antigen administered intraperitoneally, in PBS without adjuvant.

Enzyme linked Immunosorbent Assay (ELISA)

Variations of ELISA were used. Immunoadsorbant plates (Nunc Maxisorp™ 96F well plates, Thermo Fisher Scientific, 442404) were coated with a 1-5µg/ml solution of capture reagents diluted in PBS. Following repeated washing with PBST (PBS+0.05% Tween), PBS and blocking with a 3% solution of milk powder, dilutions of analyte for testing (in 3% milk powder/PBS) were applied to the plates. After washing away unbound protein, bound proteins were detected using an appropriate detection antibody solution [either directly conjugated to horseradish peroxidase (HRP) or using a biotin-mediated capture of neutravidin HRP (Pierce™, Thermo Fisher Scientific, 31030)], followed by 3,3',5,5' tetramethylbenzidine (TMB) substrate (Sigma-Aldrich, T0440), typically developed for 10 min with 0.5M H_2SO_4 (Sigma-Aldrich, 320501) applied prior to recording OD450nm. Details for various capture reagents used are described in Supplementary Materials and Methods.

Construction of phage display libraries and isolation of antigen-specific V_H antibodies

Spleen, inguinal and axillary lymph nodes were collected from immunised mice into RNAlater (Qiagen, Hilden, Germany) and mixed with 600µl of RLT buffer containing β-mercaptoethanol (Qiagen RNeasy kit, 74104) in Lysing matrix D bead tubes (MP Bio,

116913100). Tissues were homogenised in an MP Bio Fastprep homogeniser (116004500) using 6m/s 40 s cycles. Homogenised tissues were then microfuged at 16k x g for 5 min and RNA extracted from the supernatants using the Qiagen RNeasy kit. V_H genes were amplified from RNA extract by RT-PCR using Superscript III RT-PCR high-fidelity kit (Invitrogen, Thermo Fisher Scientific, 12574-035) and oligonucleotide primer V_H_J/F (long) in combination with a primer for V_H1, V_H2, V_H3, V_H4 or V_H6 family (Supplementary Table 5). V_H products at the expected molecular weight (approx. 400bp) were identified by agarose gel electrophoresis (Supplementary Figure 4a). Phagemid vector (pUCG3, Crescendo) DNA (10ng) was amplified by PCR using Phusion High Fidelity PCR master mix with GC buffer (NEB, F532L) and primers pUCG3-F3 and pUCG3-R3 (0.25µM final, Supplementary Table 6). Reactions were heated to 98ºC for 30 s and then subjected to 30 cycles of 98 ºC for 10 s; 58 ºC for 20 s; and 72ºC for 3 min. The PCR product (4.3Kb) was gel purified using Gel purification kit (Thermo Fisher Scientific, K0691). 250ng of purified V_H RT-PCR products were mixed with 700ng linearised phagemid vector and 10 cycles of PCR performed with Phusion GC as described above. V_H/phagemid PCR products were purified using PCR purification kit (Thermo Fisher Scientific, K0702) and the eluates transformed into TG1 *E. coli* (Lucigen, 60502-2) by electroporation following the manufacturer's instructions. Transformed cells were cultured on Bioassay dishes containing 2xTY agar supplemented with 2% (w/v) glucose and 100µg/ml ampicillin (2xTYAG) and incubated overnight at 30ºC. Library sizes were determined by preparing a 10-fold dilution series of each transformation and colony counting following culture on 2xTYAG petri dishes. Library quality was assessed by Sanger sequencing (GENEWIZ, Bishop's Stortford, UK) of randomly selected clones and diversity demonstrated by an analysis of V_H-CDR3 sequence length and frequency. Preparation of library phage stocks and phage display selections were performed according to published methods 0.

Expression and affinity purification of Humabody® V_H

Individual colonies from the phage selections were cultured in 1-50mL 2xTYAG broth at 37°C with 250rpm shaking. At OD600 of 0.6-1, Isopropyl β- d-1-thiogalactopyranoside (IPTG) was added to a final concentration of 1mM, and the cultures continued overnight at 30°C with shaking at 250rpm. *E. coli* cells were pelleted by centrifugation at 2200 x g for 10 mins and supernatants discarded. Cell pellets were resuspended in 1/20th volume of ice cold extraction buffer [20% (w/v) sucrose, 1mM EDTA & 50mM Tris-HCl pH8.0] for 30 min on ice and then centrifuged at 4400 x g for 15 min at 4°C. Supernatants (periplasmic extracts containing V_H) were screened directly or subjected to further purification using immobilized metal affinity chromatography (IMAC) chromatography to purify V_H *via* a C-terminal 6xHIS tag 0.

Antigen binding affinities and binding kinetics of Humabody® V_H

Binding kinetics of purified Humabody® V_H were determined on a BIAcore T200 instrument and detailed in Supplementary Materials and Methods.

IL17A and IL17RA ligand:receptor biochemical inhibition assay

Maxisorp™ mictrotitre plates were coated with 2nM IL17RA-Fc (R&D systems, 177-IR-100) overnight at 4°C. Plates were washed once with PBS and 3% Marvel/PBS added to each well to block non-specific protein interactions. Crude periplasmic extracts of Humabody® V_H were added to polypropylene plates containing 3% Marvel/PBS supplemented with 1nM recombinant IL17A, and the mixture transferred to the IL17RA-Fc coated plates for 1 h at room temperature (RT). Plates were washed 3 times each with PBST and PBS, and 0.4µg/ml of biotinylated anti-IL17A mAb (R&D Systems, BAF317) in 3% Marvel/PBS added for 1 h at RT. The PBST/PBS wash steps were repeated and then neutravidin-HRP (Pierce, 31030), diluted 1:750 in 3% Marvel/PBS, added for 1 h incubation at RT. After a final PBST/PBS wash, TMB substrate was added and incubated at RT until suitable blue colour had developed. The reaction was then stopped by addition of 0.5M H_2SO_4 and absorbances measured at 450nm in a spectrophotometer.

Biological assay for IL17A dependent secretion of IL6 by human HT1080 cells

A biological assay was developed to measure IL17A-induced IL6 release from cell line HT1080 (ECACC, 85111505). $5x10^4$ HT1080 cells/well were seeded in culture medium (MEM with Earle's salts, supplemented with non-essential amino acids, 10% fetal bovine serum (FBS), 2mM L-glutamine and penicillin/streptomycin) into a 96 flat bottomed tissue culture plate and cultured overnight. HT1080 cells were then treated with 10ng/ml of IL17A and incubated for 5 h in a humidified incubator at 37°C, 5% CO_2. The cell culture supernatant was collected and assayed for IL6 using the IL6 Duoset (R&D Systems, DY206), following manufacturer's instructions. To identify Humabody® V_H that inhibited IL17A (Figure 7e) or IL17RA (Figure 8e), serial dilutions of purified Humabody® V_H were prepared in culture medium and added to the cells together with the IL17A or pre-incubated with cells prior to the addition of IL17A respectively.

Size exclusion chromatography (SEC) of Humabody® V_H

Purified V_H proteins were analysed using a Waters 2795 Separation Module with a Waters 2487 Dual λ Absorbance Detector (Detected at 280nM) and a TSKgel G2000SWXL (TOSOH) column. Samples were injected in 10-50µl volumes and run in mobile phases of 10% isopropanol / 90% PBS at a flow rate of 0.5-0.7ml/min. Data were collected for up to 35 min and the size of the V_H fraction compared with known standards.

Results and Discussion

Design of Crescendo Mouse

The transgene engineered for Crescendo Mouse comprises human VDJ genes in their natural configuration and a truncated murine constant region, including Eμ, Cγ1 (no CH1 domain) and 3' enh region. Key to the design of the constructs was the inclusion of the entire 3' enh and the absence of Cμ and Cδ genes. A truncated or mini-3' enh have been found to be detrimental to the efficient use of Ig transgenes 0. Previous work with a small transgene

combining camelid-derived V_{HH} fragments with human C-regions has shown that IgM/IgD are not required for the expression of HC-only antibodies 0. An advantage of omitting IgM is the lack of avidity-effects caused by pentameric IgM that can enhance activity of low affinity binding sites, potentially contributing background noise and detracting from the efficient isolation of higher affinity HC-only antibody domains. In Crescendo Mouse, the murine Cγ1 gene is the only heavy chain (HC) constant gene presented in the transgene and hence the HC-only antibody isotype produced is IgG1.

Characterisation of the TKO and Crescendo human V_H transgenic mouse

In the TKO background mouse, flow cytometric examination of surface expression markers of bone marrow cells demonstrated that B cell development is arrested before the preBII stage and B cell precursors fail to progress beyond expression of the CD43 marker and a resultant blockade of Ig^+ B cell development (**Figure 2**a). In addition, spleens are greatly reduced in size within the TKO mice (Figure 2b) and exhibit an architecture consistent with an absence of B cells (Supplementary Figure 2), with few, sparsely populated follicles and no marginal zones. Within the serum, no circulating Ig can be detected (Figure 2c). Introduction of the 10V YAC transgene to the TKO background restored B cell development. Bone marrow cells of the Tg animals exhibited a grossly similar developmental marker expression to that shown by wt mice (Figure 2a). Within the periphery, spleen size was restored to that of wt (Figure 2b) with a normal architecture, displaying clear, well-populated follicular and marginal zone areas (Supplementary Figure 2). Compared with wt mice, the Tg mouse was found to have a higher proportion of splenic $CD19^+Ig^+$ cells (62.9% vs 40.1%), with the difference being due to a higher proportion of $CD19^+Ig^+CD23^-CD5^-$ B cells (**Figure 3**). However, the proportion of cells with a mature follicular B-2 B cell profile ($CD19^+Ig^+CD23^+CD5^-$) was similar in both wt and Tg mice (Figure 3). Consistent with successful reconstitution of the B cell lymphoid compartment, circulating IgG1 antibodies were readily detected in the serum of the Tg mice (Figure 2c). A splenic $CD23^{low}$ population was also observed in Ig^+ cells when camelid V_{HH} were used to generate a transgenic mouse,

particularly when the IgM genes were deleted [31]. Mice deficient in secreted IgM have been observed to have an enlarged B-1 cell compartment [32,33]. Therefore, it is conceivable that within the Crescendo Mouse, which lacks light chains, IgM and IgD, B cells may exit the bone marrow early and complete their development in the spleen giving rise to alterations in transitional B cell, marginal zone and follicular B cell subsets and the observed different staining B cell profiles [34,35].

The TKO background ensures antibodies produced in Crescendo Mouse are heavy chain only

During the process of breeding the transgene onto the TKO background, intermediate mouse lines were examined in which the endogenous HC was knocked out, but the λ or κ loci remained functional. Serum ELISA experiments showed that endogenous LCs could be associated with the IgHCs encoded by the introduced transgene (Figure 4). The results indicated a critical role for the knockout of all endogenous Ig chains to obtain HC-only antibody expression using the human V_H genes. The association of LC and transgene HC occurred in the absence of the CH1 domain and may be mediated by a disulphide bond between the cysteine in the LC C-terminal and cysteine in the HC hinge region. A non-covalent interaction between the V_H and LC is also possible since a V_H domain N2D5 (see Figure 9) is still capable of binding both κ and λ LCs. In the TKO background, however, B cells expressed HC-only antibodies matured in the absence of LCs. Hence only V_H that are intrinsically stable can be expressed and displayed on the B cells, thus providing an *in vivo* "filter" to preclude development of unstable V_H.

Naïve Crescendo Mouse produces a highly diverse HC-Ab repertoire

The sequences of Humabody® V_H isolated from naïve Tg mice were analysed and all 10 V_H gene segments encoded by the transgene were shown to give rise to HC-only antibodies at different frequencies (**Figure 5**a). Moreover, all 6 human J_H genes were also utilised (Figure 5b) and V_H CDR3 diversity was extensive with sequence lengths ranging from 3 to 27 amino

acids (Figure 5c). Consistent with the naïve status of the mouse, isolated sequences were largely germline with little evidence of mutation within the framework (FR) or CDR1 or CDR2 regions (Supplementary Figure 3a). Thus, within the naïve Tg mouse, framework mutations are not required to support the development of B cells expressing HC-only antibodies using a diverse range of human V_H genes. This observation is consistent with the lack of activation-induced cytidine deaminase function observed during B cell development in the bone marrow 0. Therefore, mutations such as the germline changes described in the FR2 of camelid V_{HH} 0, postulated to play a role in stabilising camelid V_{HH} expression, were not required for efficient human V_H expression in the Crescendo Mouse. Within camelids, HC-only antibodies are co-expressed with conventional H_2L_2 antibodies 0, and thus these "camelising residues" may actually serve to protect V_{HH} from association with endogenous LCs. The naïve Crescendo Mouse developed a repertoire of HC antibodies utilising all 10 V_H genes of five V_H families that were available, including families previously shown to have poor biophysical properties as isolated domains 0. This is in contrast to camelid V_{HH} which are of V_H3 or V_H4 origin 0, and also human *in vitro* V_H domain libraries where successes have been limited to V_H3 families [14,40]. *In vitro* libraries have been further designed to promote V_H stability but have required extensive engineering in either the CDR 0 or framework regions 0. Unlike these empirical *in vitro* studies, Crescendo Mouse exemplifies the powerful *in vivo* selection processes that create an immune repertoire from the many millions of theoretical solutions using a broad range of human germline genes, supporting the progression of effective solutions for *in vivo* V_H development.

Robust platform for rapid isolation of Humabody® V_H candidates

The Crescendo Mouse exhibits robust HC-Ab responses to immunisation with a variety of antigens (**Figure 6**). Following immunisations with IL17A (Figures 6c, 6d) and IL17RA (Figures 6e, 6f), V_H sequences were determined from the spleen and draining lymph nodes and separate phage display libraries constructed from each mouse (IL17A, supplementary Figure 4). A single round of phage display selection was then performed to enrich for

antigen-reactive Humabody® V_H (**Figure 7**a, **Figure 8**a). Screening by ELISA of samples from the selected libraries revealed a panel of Humabody® V_H with binding activity for both targets (Figures 7b, 8b). A ligand:receptor assay was developed to screen for Humabody® V_H that disrupted binding of recombinant IL17A to IL17RA (see Materials and Methods). For Humabody® V_H with strong antagonistic activity, 66 were identified for IL17A and 335 for IL17RA. Sequence analysis revealed that 58 of the 66 IL17A clones, and 177 of the 335 IL17RA clones, were unique.

Following immunisation, the Crescendo Mouse mounted strong HC-only antibody responses and mutations were apparent as a result of normal somatic hypermutation process within germinal centres. These mutations were observed throughout the V_H sequence with both framework and CDR regions affected (supplementary Figures 3, 5 and 6), a finding in keeping with observations in conventional antibodies [43,44]. In addition, the average Humabody® V_H CDR3 sequence length was 14.5 amino acid residues in range of 3-27, a figure also consistent with that for conventional human antibodies (average of 15 in range of 4-32) [43,45-47]. Extended CDR3 sequences, commonly described in camelid V_{HH} [41,48], were not recapitulated in Humabody® V_H. Similarly, single cysteine residues in CDR1 and CDR3, described in some camelid V_{HH} and postulated to promote stability by additional disulphide bridging 0 were not observed in Humabody® V_H. However, some Humabody® V_H fragments were identified with 2 cysteine residues in the CDR3, one example being reported here (anti-IL17RA V_H, 5D6, CDR3 sequence EKGLGFCRGGSCSYFDY, supplementary Figure 6b). Similar double cysteine-containing CDR3 sequences have been reported in human antibodies 0, and were shown to form disulphide bridges that were important for antibody activity 0. These observations suggest that the sequences of Humabody® V_H are more closely aligned to conventional human antibodies than to camelid V_{HH}. However, closer examination of 20,000 naïve Humabody® V_H CDR3 sequences did identify an increase in aspartic acid frequency compared to that reported in human antibodies 0 (Supplementary Figure 7). Aspartic acid residues have been reported in other V_H domain and scFv libraries

and shown to confer the favourable biophysical property of non-aggregation [51,52]. The presence of charged and polar uncharged residues has been observed with increased frequency in the CDR3 of HC-Abs from the UniRat platform compared to H_2L_2 antibodies 0. Thus, acidification in V_H CDR3 may be one of the mechanisms employed by the Crescendo Mouse to generate functional and stable single domain V_H antibodies.

High affinity Humabody® V_H with therapeutic potency

Monomeric antagonist Humabody® V_H isolated directly from the mouse typically have affinities in the low nM to pM range, e.g. 53F9 (anti-IL17A, 3nM), 56H4 (anti-IL17RA, 6nM), and 5D6 (anti-IL17RA, 60pM) (Figure 7c, Figure 8c). 53F9 and 56H4 are members of larger families of related antagonists (Supplementary Figures 5, 6) and represent a blueprint (map of hot spots) of the somatic hypermutation (SHM) processes that occurred during the immune response. These blueprints were used to inform sequence choices, incorporating alternative amino acids at the mutational “hot spots” (highlighted in supplementary Figures 5, 6), into new phage display libraries that were successfully interrogated to identify new variants of 53F9 and 56H4 with significantly improved affinities: 73E2 (600pM) and 78E10 (500pM) for IL17A, and 84A4 (1.5nM) for IL17RA. In addition to their high affinities, the IL17A and IL17RA neutralising Humabody® V_H demonstrated exquisite specificity for their target, failing to bind alternative closely related family members, but showing species cross-reactivity with cynomolgus monkey and, in the case of the IL17A antagonists, porcine homologous proteins (Figure 7d, Figure 8d). The antagonists were also screened in a biologically relevant assay and shown to prevent IL17A-dependent secretion of IL6 by HT1080 cells, with potencies in the low nM range (Figure 7e, Figure 8e).

Humabody® V_H candidates with superior biophysical properties

A key requirement of any therapeutic is that it has good biophysical properties and is amenable to development. Natural human V_H domains derived from a conventional H_2L_2 antibody format have been studied without their partner light chain and typically have poor

expression properties and a tendency to aggregate [38,53]. V_H domains from human spleen cDNA (Clontech) and from naïve Crescendo Mouse were cloned into the phagemid vector for expression and purification (Supplementary material). A total of 34 V_H from human spleen were expressed (7 from the V_H1 family, 6 V_H2, 8 V_H3, 7 V_H4 and 6 V_H6) and compared with 32 Humabody® V_H from the Crescendo Mouse (7 V_H1, 5 V_H2, 8 V_H3, 7 V_H4 and 5 V_H6). Yields of purified protein were determined by OD280 measurement. Humabody® V_H showed 4-fold higher expression yields compared to V_H isolated from conventional H_2L_2 antibodies, indicative of favourable biophysical properties. Indeed, after initial screening with phagemid vector, expression yields of Humabody® V_H in *E. coli* are typically above 50 mgL^{-1} in an expression vector with terrific broth in shake flask cultures and >10gL^{-1} has been achieved by fermentation (data not shown). In addition to high levels of expression, the neutralising Humabody® V_H described here exhibited no propensity to aggregate and remained monomeric, as determined by size exclusion chromatography (Figure 7f, Figure 8f), and no association with free LCs was demonstrated by ELISA (**Figure 9**).

Thus, the Crescendo Mouse generates Humabody® V_H that remain stable as monomeric domains and offers excellent development opportunities for the manufacture of small bio-therapeutics. The repertoire of the Crescendo Mouse was mined as a population, there being no need to maintain cognate light and heavy chain pairings used at the single B cell level in a conventional Ig response. This means that discovery techniques such as hybridoma generation or single cell sorting [54] are not required for the platform. Moreover, the genes for the V_H were harvested directly, rather than retaining the chimeric HC format. This meant that the discovery proceeded rapidly and efficiently using the final format or module of the proposed therapeutic. We also employed sequencing to map hot-spots of affinity maturation and produce sequence blueprints of the germinal centre, leveraging this information to further improve V_H affinities and retaining the enhanced biophysical properties by recombining mutations identified by the mouse.

Conclusions

Antibody V_H fragments have emerged as an important new class of small, potent biotherapeutics with advantages for multiple routes of administration, improved tissue and tumour penetration, engineering of multispecific and multifunctional products, and simple manufacture [55,56]. Here, a new mouse platform is described, the Crescendo Mouse, with human VDJ genes in conjunction with mouse Cγ1 lacking CH1 domain joined to a full mouse 3' enh, generating HC-only antibodies in a background devoid of endogenous immunoglobulin expression. The Crescendo Mouse has an extensive B cell repertoire and developmental pathway resulting in healthy immunocompetent mice able to mount robust acquired immune reactions to various antigens. That the omission of IgM does not unduly limit the choice of candidates for *in vivo* affinity maturation is demonstrated here both at the sequence level and by the isolation of potent Humabody® V_H antagonists to human IL17A and IL17RA with therapeutic potential for the treatment of Th17 associated pathologies 0. The Crescendo Mouse provides a robust platform for rapidly developing potent Humabody® therapeutics for unmet medical need.

Acknowledgements

We would like to thank Dr Marianne Brüggemann for her critical discussion and input in YAC construction, Dr Robert Norrington and Dr Sue Edwards and team (Charles River Laboratories) for platform maintenance, Dr Will Howat (Abcam plc) for IHC imaging and Dr Anne Sigonds-Pichon (Babraham Institute) for statistical analysis of amino acid usage.

Conflicts of interest

The authors declare no conflicts in interest.

AUTHOR CONTRIBUTIONS

JLY, BE and YT wrote the manuscript. JLY, BE, YT, PH, LT, CE, YS, CJ, MW, DP, YZ, MR(Roode), PC, LM, AF, BR, VT, and KG performed research. AEC, CB and LM analyzed

data. JLY, BE, YT, BMcG, TS and MR(Romanos) designed research. All authors read and approved the final manuscript.

LEGENDS TO FIGURES

Figure 1: Construction of YACs and transgenic founders. Diagrammatic (not to scale) representations of (a) the conversion of a BAC encoding human heavy chain variable genes into YACa; (b) joining of two YACs (YACa and sYAC) into a single YAC containing 10 human V_H genes by bridge-induced translocation; (c) the addition of murine Cγ1 region with CH1 exon deletion (mC) plus other regulatory elements (murine Eμ plus murine 3' enh region) to YACb by recombination in yeast; (d) the final 10V YAC construct used for transgenesis; (e) metrics of microinjection and transgenesis results. (TRP, LEU, ADE, URA, LYS and HIS are yeast auxotrophic selection markers *TRP1, LEU2, ADE2, URA3, LYS2* and *HIS3*, respectively; V/D/J: human Ig heavy chain V/D/J genes; Cen: centromere; Eμ: μ enhancer; Sμ: μ switch region; hC: human IgH constant gene γ4 without CH1; mC: murine IgH constant gene γ1 without CH1; L1-4: Linker 1-4; K: kanamycin resistance gene; Hyg: Hygromycin resistance gene; m3'E: murine 3' enhancer; open circle: centromere; solid arrow: telomere).

Figure 1. Construction of YACs and creation of transgenic founders

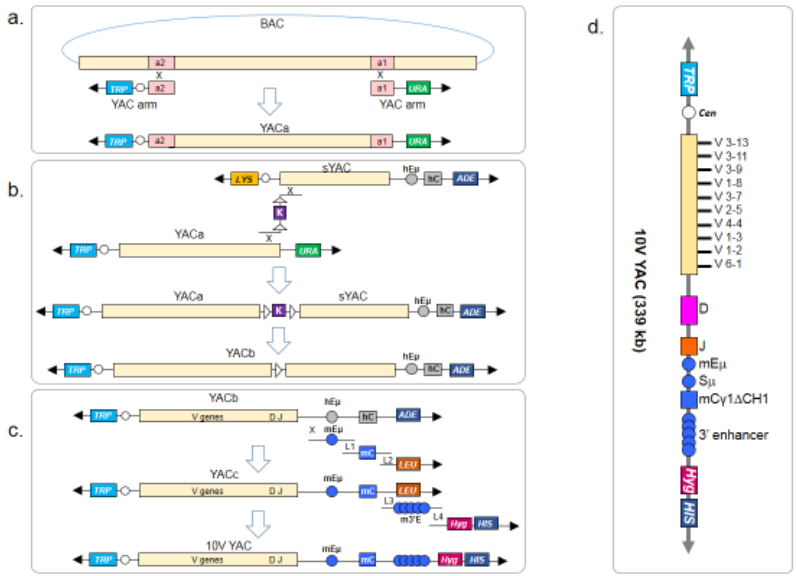

e.

Transgenic process	Microinjection # sessions	# oocytes injected	# oocytes transferred	# pseudo-pregnant recipients	# pups delivered	# pups analyzed	Screen Results # positive
	10	834	562	26	67	57	7 (6 partial)

Figure 2: B cell development was reconstituted in the Crescendo Mouse. (a) Flow cytometric analysis of bone marrow cells stained with anti-B220 antibody (horizontal axis) and antibodies to differentiation markers (vertical axis), CD117, CD43, Ly51, CD25, IgM-Fc (TKO & wt) or IgG-Fc (Crescendo Mouse); (b) photograph of spleens from wild type mouse, TKO mouse and Crescendo Mouse; (c) sandwich ELISA detecting serum Ig Fcγ chains in TKO (circles), wild type (squares) and the Crescendo Mouse (triangles).

Figure 2. B cell development is reconstituted in the Crescendo Mouse

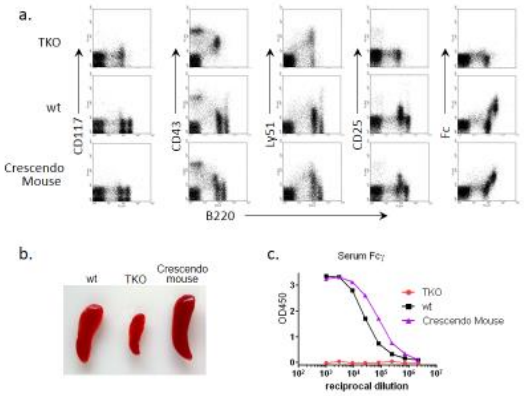

Figure 3: Flow cytometry analysis of spleen cells using antibodies to CD19, IgM-Fc (wt) or IgG-Fc (Crescendo Mouse), CD5 and CD23. Live cells were gated using FSC v SSC plots (not shown) and further gating is indicated by each plot.

Figure 3. Flow cytometry analysis of splenic cells using antibodies to CD19, IgM-Fc (wt) or IgG-Fc (Crescendo Mouse), CD5 and CD.

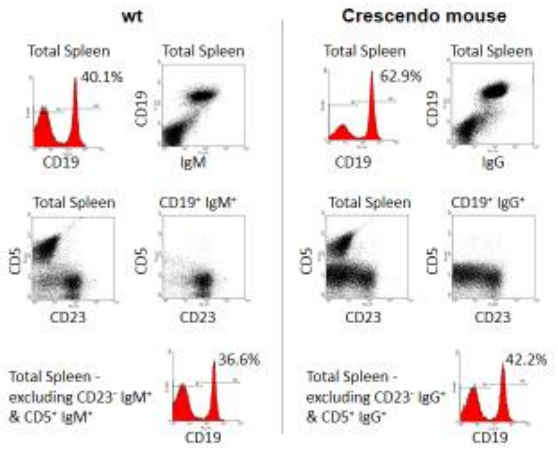

Figure 4: Sandwich ELISA detecting heavy and light chain associations in the sera of transgenic mice. Serum samples from Tg mice carrying the 10V YAC transgene on a TKO background (Crescendo Mouse), or on a background with endogenous κ chain ($\kappa^{+/-}$) or λ chain ($\lambda^{+/-}$) were tested in paired sandwich ELISA (n=3 for each test, mean +/- SD are plotted). The presence (+) or absence (-) of genes is noted for each mouse. Antibody in mouse serum was captured with goat anti-mouse IgG (Fcγ fragment specific, Jackson, 115-005-164) and detected with biotinylated sheep anti-mouse IgG (Amersham, RPN1001) for HC, and with biotinylated goat anti-mouse IgG (light chain specific, Jachson, 115-065-174) for HC associated κ or λ L chains. Bound biotinylated proteins were detected by neutravidin HRP and TMB substrate reaction.

Figure 4. Sandwich ELISA detecting heavy and light chain associations in the serum of transgenic mice.

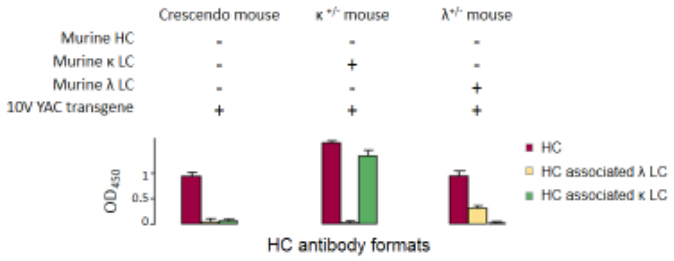

Figure 5: V_H sequence analysis of naïve Crescendo Mouse. Deep sequencing analysis showing: (a) utilisation of human V_H germline gene segments (IGHV) and (b) human J_H gene segments (IGHJ) in the Crescendo Mouse according to IMGT nomenclature (bone marrow proB cells from 2 individual mice); (c) length distribution analysis of 344036 unique Humabody® V_H CDR3 sequences derived from spleens of 113 naïve mice (CDR3 analysis by CLC Workbench software, Qiagen. IMGT nomenclature, http://www.imgt.org).

Figure 5. V_H Sequence analysis of Naïve Crescendo Mouse

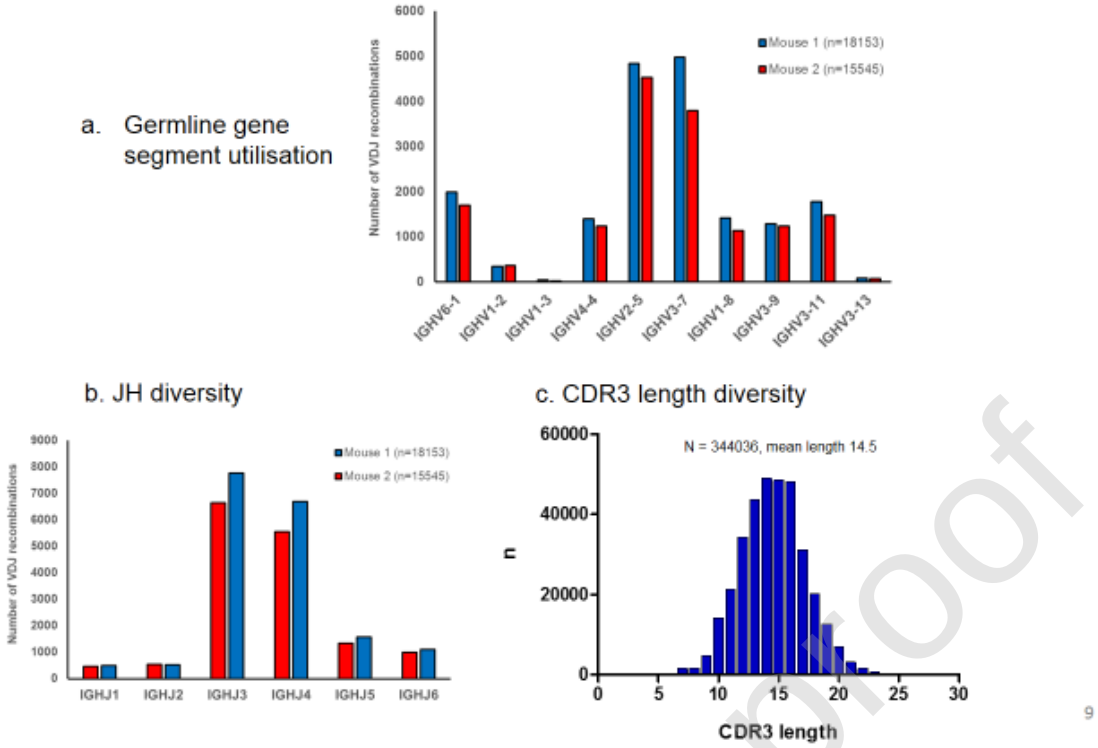

Figure 5. V_H Sequence analysis of Naïve Crescendo Mouse

Figure 6: HC-Ab responses following immunisation of Crescendo Mouse. Serum samples from immunised mice were titrated in ELISA against target antigens to measure antibody production in post-immune (closed symbols) and pre-immune (open symbols) mice. (a) KLH 28 day immunisation; (b) ovalbumin 49 day immunisation; (c) human IL17A 28 day immunisation; (d) human IL17A 49 day immunisation; (e) and (f) human IL17RA 49 day immunisations.

Figure 6. HCAb responses following immunisation of Crescendo mouse

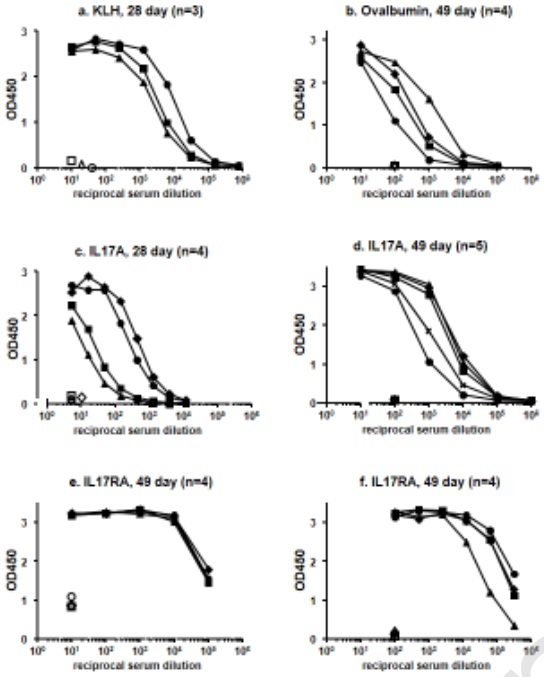

Figure 7: Discovery of antagonistic IL17A-specific Humabody® V_H. (a) Discovery process for 5 mice immunised with human IL17A, illustrating phage library sizes pre- and post-selection on human IL17A and the metrics for isolating neutralising V_H fragments with unique CDR3 sequences; (b) ELISA screening of multiple V_H clones from each mouse measuring Humabody® V_H binding to human IL17A following phage display selections; (c) single cycle kinetics traces (sensorgrams) generated on a BIAcore T200 instrument measuring binding affinities of Humabody® V_H for human IL17A (Supplementary Materials and Methods); (d) ELISA to measure binding of Humabody® V_H 53F9, 73E2, 78E10, or 86A5 (KLH-specific Humabody® V_H control) to human, porcine and cynomologus monkey IL17A, human IL17A/F heterodimer, other IL17 family members or control proteins (IgG, KLH) (n=3 for each assay point, mean +/- SD are plotted); (e) HT1080 cell based assay to demonstrate inhibition of IL17A-dependent production of IL6 by Humabody® V_H 53F9 (square), 73E2 (triangle), 78E10

(inverted triangle) or an irrelevant control (diamond); (f) size exclusion chromatography traces of purified Humabody® V_H.

Figure 7. Discovery of antagonistic IL17A-specific Humabody® V_H

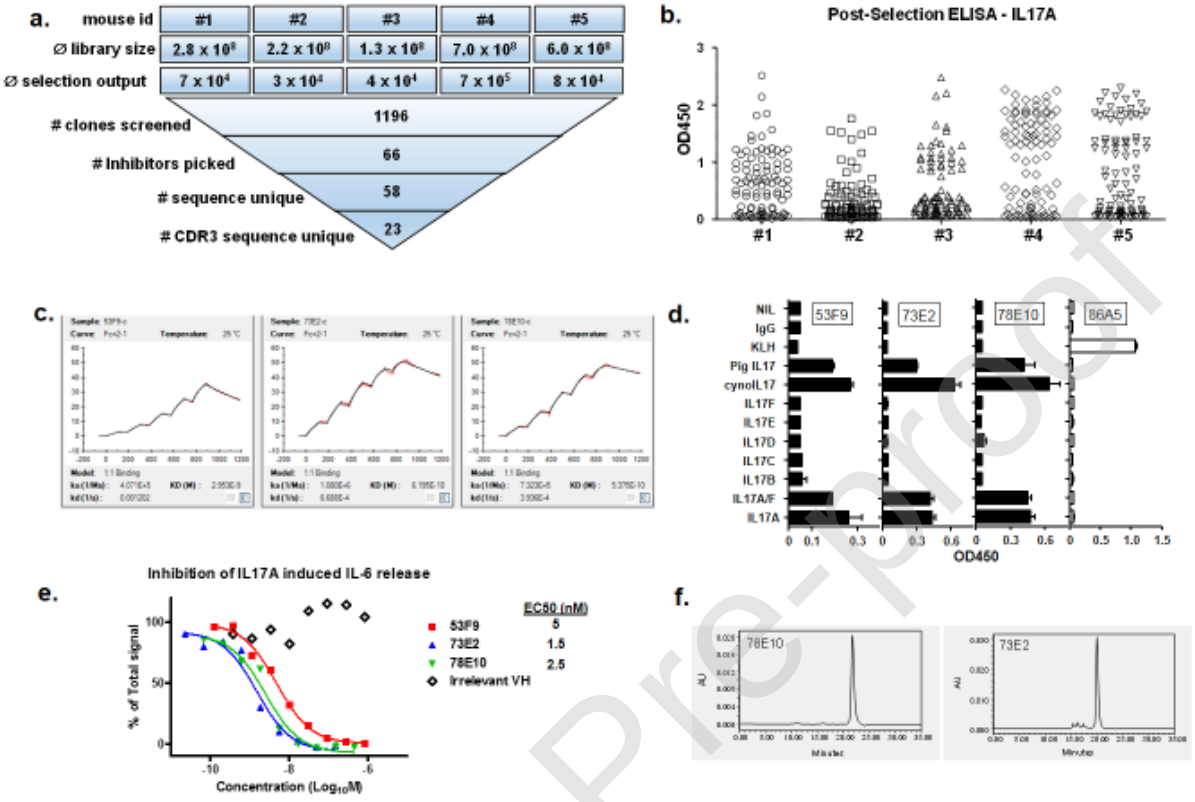

Figure 8: Discovery of antagonistic IL17RA-specific Humabody® V_H. (a) Discovery process for 4 mice immunised with human IL17RA, illustrating phage library sizes pre- and post-selection on human IL17RA and the metrics for isolating neutralising V_H with unique CDR3 sequences; (b) ELISA screening of multiple V_H clones from each mouse measuring Humabody® V_H binding to human IL17RA following phage display selections; (c) single cycle kinetics traces generated on a BIAcore T200 instrument measuring binding affinities of Humabody® V_H for human IL17RA; (d) ELISA to measure binding of Humabody® V_H clones 56H4, 84A4, 5D6 or 86A5 (KLH specific Humabody® V_H control) to human and cynomologus monkey IL17RA, other members of the IL17R family and control proteins (OVA: ovalbumin,

HEL: Hen Egg Lysozyme, IgG, KLH) (n=3 for each assay point, mean +/- SD are plotted); (e) HT1080 cell based assay to demonstrate inhibition of IL17A-dependent production of IL6 by Humabody® V_H 56H4 (square), 84A4 (triangle), 5D6 (inverted triangle) or an irrelevant control (diamond); (f) size exclusion chromatography traces of purified Humabody® V_H.

Figure 8. Discovery of antagonistic IL17RA-specific Humabody® V_H

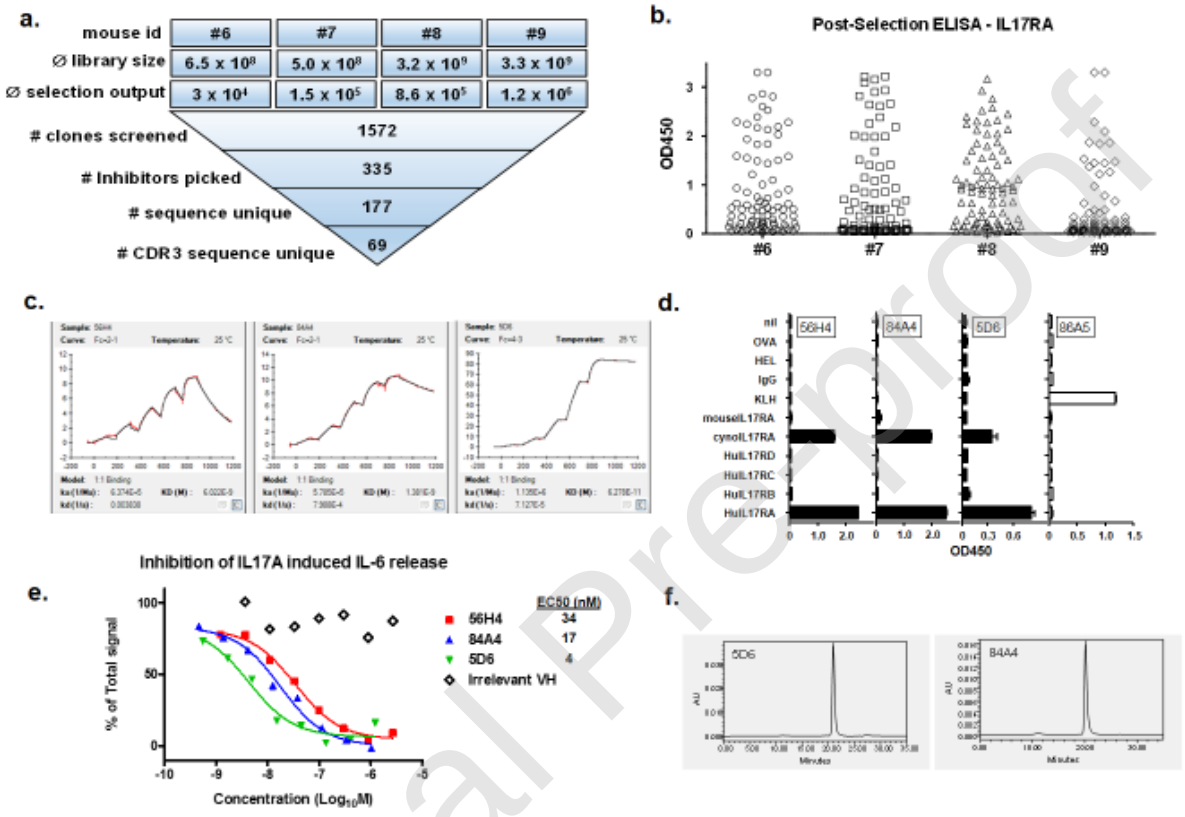

Figure 9: Panel of Humabody® V_H leads shows no association with free light chains. Direct binding ELISA demonstrates Humabody® V_H (53F9, 73E2, 78E10, 56H4, 84A4 and 5D6) did not bind free light chains. A V_H domain isolated from human splenic cDNA, N2D5, was included as positive control.

Figure 9: Panel of Humabody® V_H show no association with free light chains.

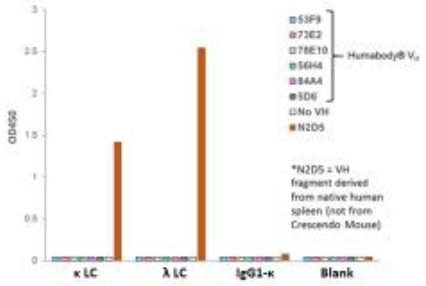

References

[1] Grilo AL, Mantalaris A. The Increasingly Human and Profitable Monoclonal Antibody Market. Trends Biotechnol. 2019; 37:9-16. doi: 10.1016/j.tibtech.2018.05.014.

[2] Brüggemann M, Caskey HM, Teale C, Waldmann H, Williams GT, Surani MA, *et al.* A repertoire of monoclonal antibodies with human heavy chains from transgenic mice. Proc Natl Acad Sci USA. 1989; 86:6709-13.

[3] Lonberg N, Taylor LD, Harding FA, Trounstine M, Higgins KM, Schramm SR, *et al.* Antigen-specific human antibodies from mice comprising four distinct genetic modifications. Nature. 1994; 368:856-9.

[4] Macdonald LE, Karow M, Stevens S, Auerbach W, Poueymirou WT, Yasenchak J, *et al.* Precise and in situ genetic humanization of 6 Mb of mouse immunoglobulin genes. Proc Natl Acad Sci USA. 2014; 111:5147-52. doi: 10.1073/pnas.1323896111.

[5] Murphy AJ, Macdonald LE, Stevens S, Karow M, Dore AT, Pobursky K, *et al.* Mice with megabase humanization of their immunoglobulin genes generate antibodies as efficiently as normal mice. Proc Natl Acad Sci USA. 2014; 111:5153-8. doi: 10.1073/pnas.1324022111.

[6] Lee EC, Liang Q, Ali H, Bayliss L, Beasley A, Bloomfield-Gerdes T, *et al.* Complete humanization of the mouse immunoglobulin loci enables efficient therapeutic antibody discovery. Nat Biotechnol. 2014; 32:356-63. doi: 10.1038/nbt.2825.

[7] Osborn MJ, Ma B, Avis S, Binnie A, Dilley J, Yang X, *et al.* High-affinity IgG antibodies develop naturally in Ig-knockout rats carrying germline human IgH/Igκ/Igλ loci bearing the rat CH region. J Immunol. 2013; 190:1481-90. doi: 10.4049/jimmunol.1203041.

[8] Ma B, Osborn MJ, Avis S, Ouisse LH, Ménoret S, Anegon I, *et al.* Human antibody expression in transgenic rats: Comparison of chimeric IgH loci with human V_H, D and J_H but

bearing different rat C-gene regions. J Immunol Methods. 2013; 400-401:78-86. doi: 10.1016/j.jim.2013.10.007.

[9] Chen WC, Murawsky CM. Strategies for Generating Diverse Antibody Repertoires Using Transgenic Animals Expressing Human Antibodies. Front Immunol. 2018; 9:460. doi: 10.3389/fimmu.2018.00460.

[10] Xenaki KT, Oliveira S, van Bergen En Henegouwen PMP. Antibody or Antibody Fragments: Implications for Molecular Imaging and Targeted Therapy of Solid Tumors. Front Immunol. 2017; 8:1287. doi: 10.3389/fimmu.2017.01287.

[11] Taussig MJ, Stoevesandt O, Borrebaeck CA, Bradbury AR, Cahill D, Cambillau C, *et al.* ProteomeBinders: planning a European resource of affinity reagents for analysis of the human proteome. Nature Methods. 2007; 4:13-7.

[12] Bates A, Power CA. David vs. Goliath: The Structure, Function, and Clinical Prospects of Antibody Fragments. Antibodies. 2019; 8:28. doi.org/10.3390/antib8020028.

[13] Kholodenko RV, Kalinovsky DV, Doronin II, Ponomarev ED, Kholodenko IV. Antibody Fragments as Potential Biopharmaceuticals for Cancer Therapy: Success and Limitations. Curr Med Chem. 2019; 26:396-426. doi: 10.2174/0929867324666170817152554.

[14] Holt LJ, Herring C, Jespers LS, Woolven BP, Tomlinson IM. Domain antibodies: proteins for therapy. Trends Biotechnol. 2003; 21:484-90.

[15] Hamers-Casterman C, Atarhouch T, Muyldermans S, Robinson G, Hamers C, Songa EB, *et al.* Naturally occurring antibodies devoid of light chains. Nature 363, 446-8 (1993).

[16] Muyldermans, S. Nanobodies: natural single-domain antibodies. Annu Rev Biochem. 2013; 82:775-97. doi: 10.1146/annurev-biochem-063011-092449.

[17] Clarke SC, Ma B, Trinklein ND, Schellenberger U, Osborn MJ, Ouisse LH, *et al.* Multispecific Antibody Development Platform Based on Human Heavy Chain Antibodies. Front Immunol. 2019; 9:3037. doi: 10.3389/fimmu.2018.03037.

[18] Bannas P, Hambach J, Koch-Nolte F. Nanobodies and Nanobody-Based Human Heavy Chain Antibodies As Antitumor Therapeutics. Front Immunol. 2017; 8:1603. doi: 10.3389/fimmu.2017.01603.

[19] Khodabakhsh F, Behdani M, Rami A, Kazemi-Lomedasht F. Single-Domain Antibodies or Nanobodies: A Class of Next-Generation Antibodies. Int Rev Immunol. 2018; 37:316-22. doi: 10.1080/08830185.2018.1526932.

[20] Kouprina N, Noskov VN, Larionov V. Selective Isolation of Large Chromosomal Regions by Transformation-Associated Recombination Cloning for Structural and Functional Analysis of Mammalian Genomes. YAC Protocols, Second Edition, Humana Press Inc (Totowa, New Jersey). 85-102 (2006).

[21] Tosato V, West N, Zrimec J, Nikitin DV, Del Sal G, Marano R, *et al.* Bridge-Induced Translocation between NUP145 and TOP2 Yeast Genes Models the Genetic Fusion between the Human Orthologs Associated With Acute Myeloid Leukemia. Front Oncol. 2017; 7:231. doi: 10.3389/fonc.2017.00231.

[22] Gibson DG, Benders GA, Axelrod KC, Zaveri J, Algire MA, Moodie M, *et al.* One-step assembly in yeast of 25 overlapping DNA fragments to form a complete synthetic Mycoplasma genitalium genome. Proc Natl Acad Sci USA. 2008; 105:20404-9. doi: 10.1073/pnas.0811011106.

[23] Sanchez CP, Lanzer M. Construction of yeast artificial chromosome libraries from pathogens and nonmodel organisms. Methods Mol Biol. 2006; 349:13-26.

[24] Fernandez A, Munoz D, Montoliu L. Generation of Transgenic Animals by Use of YACs. Advanced Protocols for Animal Transgenesis. Shirley Pease & Thomas L. Saunders. Springer Protocols, 2011; 137-58.

[25] Ren L, Zou X, Smith JA, Brüggemann M. Silencing of the immunoglobulin heavy chain locus by removal of all eight constant-region genes in a 200-kb region. Genomics. 2004; 84;686-95.

[26] Zou X, Piper TA, Smith JA, Allen ND, Xian J, Brüggemann M. Block in Development at the Pre-B-II to Immature B Cell Stage in Mice Without Ig kappa and Ig lambda light chain. J Immunol. 2003; 170:1354-61.

[27] Zou X, Xian J, Popov AV, Rosewell IR, Müller M, Brüggemann M. Subtle differences in antibody responses and hypermutation of lambda light chains in mice with a disrupted chi constant region. Eur J Immunol. 1995; 25:2154-62.

[28] Bolland DJ, Koohy H, Wood AL, Matheson LS, Krueger F, Stubbington MJ, *et al.* Two Mutually Exclusive Local Chromatin States Drive Efficient V(D)J Recombination. Cell Rep. 2016; 15:2475–87. doi: 10.1016/j.celrep.2016.05.020.

[29] Benny KC Lo (Editor). Antibody Engineering. Methods in Mol Biology. 2004; 248:161-76. Doi: 10.1385/1592596665.

[30] Young CL, Britton ZT, Robinson AS. Recombinant protein expression and purification: a comprehensive review of affinity tags and microbial applications. Biotechnol.J. 2012; 7:620-34. doi: 10.1002/biot.201100155.

[31] Janssens R, Dekker S, Hendriks RW, Panayotou G, van Remoortere A, San JK, *et al.* Generation of heavy-chain-only antibodies in mice. Proc Natl Acad Sci USA. 2006; 103:15130-35.

[32] Deenen GJ, Kroese FG. Murine peritoneal Ly-1 B cells do not turn over rapidly. Ann NY Acad Sci. 1992; 651:70-71.

[33] Boes M, Esau C, Fischer MB, Schmidt T, Carrol M, Chen J. Enhanced B-1 cell development, but impaired IgG antibody responses in mice deficient in secreted IgM. J Immunol. 1998; 160:4776-57.

[34] Allman D, Pillai S. Peripheral B cell Subsets. Curr Opin Immunol. 2008; 20:149-57.

[35] Allman D, Lindsley RC, DeMuth W, Rudd K, Shinton SA, Hardy RR. Resolution of three nonproliferative immature splenic B cell subsets reveals multiple selection points during peripheral B cell maturation. J Immunol. 2001; 167:6834–40.

[36] Hwang JK, Alt FW, Yeap LS. Related Mechanisms of Antibody Somatic Hypermutaton and Class Switch recombination. Microbiol Spectr. 2015; 3:MDNA3-0037-2014. doi: 10.1128/microbiolspec.MDNA3-0037-2014.

[37] Muyldermans S, Atarhouch T, Saldanha J, Barbosa JA, Hamers R. Sequence and structure of V_H domain from naturally occurring camel heavy chain immunoglobulins lacking light chains. Protein Eng. 1994; 7:1129-35.

[38] Ewert S, Huber T, Honegger A, Plückthun A. Biophysical properties of human antibody variable domains. J Mol Biol. 2003; 325:531-53.

[39] Deschacht N, De Groeve K, Vincke C, Raes G, De Baetselier P and Muyldermans S. A novel promiscuous class of camelid single-domain antibody contributes to the antigen-binding repertoire. J Immunol. 2010; 184(10):5696-704. doi: 10.4049/jimmunol.0903722.

[40] Chen W, Zhu Z, Feng Y, Xiao X, Dimitrov DS. Construction of a large phage-displayed human antibody domain library with a scaffold based on a newly identified highly soluble, stable heavy chain variable domain. J Mol Biol. 2008; 382:779-89. doi: 10.1016/j.jmb.2008.07.054.

[41] Rouet R, Dudgeon K, Christie M, Langley D, Christ D. Fully Human V_H Single Domains That Rival the Stability and Cleft Recognition of Camelid Antibodies. J Biol Chem. 2015; 290:11905-17. doi: 10.1074/jbc.M114.614842.

[42] Barthelemy PA, Raab H, Appleton BA, Bond CJ, Wu P, Wiesmann C, Sidhu SS. Comprehensive analysis of the factors contributing to the stability and solubility of autonomous human V_H domains. J Biol Chem. 2008; 283:3639-54.

[43] Shi B, Ma L, He X, Wang X, Wang P, Zhou L, *et al.* Comparative analysis of human and mouse immunoglobulin variable heavy regions from IMGT/LIGM-DB with IMGT/HighV-QUEST. Theor Biol Med Model. 2014; 11:30. doi: 10.1186/1742-4682-11-30.

[44] Lloyd C, Lowe D, Edwards B, Welsh F, Dilks T, Hardman C *et al.* Modelling the human immune response: performance of a 10^{11} human antibody repertoire against a broad panel of therapeutically relevant antigens. Protein Eng Des Sel. 2009; 22:159-168. doi.org/10.1093/protein/gzn058.

[45] Wu TT, Johnson G, Kabat EA. Length distribution of CDRH3 in antibodies. Proteins. 1993; 16:1–7.

[46] Brezinschek HP, Foster SJ, Brezinschek RI, Dörner T, Domiati-Saad R, Lipsky PE. Analysis of the human V_H gene repertoire. Differential effects of selection and somatic hypermutation on human peripheral CD5(+)/IgM+ and CD5(-)/IgM+ B cells. J Clin Invest. 1997; 99:2488–501.

[47] Arnaout, R. et al. High-Resolution Description of Antibody Heavy-Chain Repertoires in Humans. PLoS One. 2011; 6(8):e22365 (2011). doi:10.1371/journal.pone.0022365.

[48] Desmyter A, Transue TR, Ghahroudi MA, Thi MH, Poortmans F, Hamers R, *et al.* Crystal structure of a camel single-domain V_H antibody fragment in complex with lysozyme. Nat Struct Biol. 1996; 9:803-11.

[49] Griffiths AD, Malmqvist M, Marks JD, Bye JM, Embleton MJ, McCafferty J, *et al.* Human anti-self antibodies with high specificity from phage display libraries. EMBO J. 1993; 12:725-34.

[50] Almagro JC, Raghunathan G, Beil E, Janecki DJ, Chen Q, Dinh T, *et al.* Characterization of a high-affinity human antibody with a disulfide bridge in the third complementarity-determining region of the heavy chain. J Mol Recognit. 2012; 25:125-35. doi: 10.1002/jmr.1168.

[51] Arbabi-Ghahroudi M, To R, Gaudette N, Hirama T, Ding W, MacKenzie R, Tanha J. Aggregation-resistant V_Hs selected by *in vitro* evolution tend to have disulfide-bonded loops and acidic isoelectric points. Protein Eng Des Sel. 2009; 22:59-66. doi: 10.1093/protein/gzn071.

[52] Dudgeon K, Rouet R, Kokmeijer I, Schofield P, Stolp J, Langley D, *et al.* General strategy for the generation of human antibody variable domains with increased aggregation resistance. Proc Natl Acad Sci USA. 2012; 109:10879-84. doi: 10.1073/pnas.1202866109.

[53] Lowe D, Dudgeon K, Rouet R, Schofield P, Jermutus L, Christ D. Aggregation, stability, and formulation of human antibody therapeutics. Adv Protein Chem Struct Biol. 2011; 84:41-61. doi: 10.1016/B978-0-12-386483-3.00004-5.

[54] Tiller, T. Single B cell antibody technologies. Nat Biotechnol. 2011; 28:453-7. doi: 10.1016/j.nbt.2011.03.014.

[55] Harmsen MM, De Haard HJ. Properties, production, and applications of camelid single-domain antibody fragments. Appl Microbiol Biotechnol. 2007; 77:13-22.

[56] Nelson AL. Antibody fragments - Hope and hype. MAbs. 2010; 2:77–83.

[57] Gaggen SL, Jain R, Garg AV, Cua DJ. The IL23-IL17 immune axis: from mechanisms to therapeutic testing. Nat Rev Immunol. 2014; 14:585-600. doi: 10.1038/nri3707.